

545689

**Sandia National Laboratories**Operated for the U.S. Department of Energy by
Sandia Corporation4100 National Parks Highway
Carlsbad, NM 88220Phone: (505) 234-0005
Fax: (505) 234-0061
Internet: mbnemer@sandia.gov**Martin B. Nemer, PhD**
Senior Member of Technical Staff

Date: February 08, 2007

To: WIPP SNL Records Center

Technical Review: Eric Vugrin, 6711

QA Review: Mario Chavez, 6710

Management Review: Moo Lee, 6711

Effects of not including emplacement materials in CPR inventory on recent PA results

In recent planning discussions with the U. S. Environmental Protection Agency (EPA), the EPA stated that the U. S. Department of Energy (DOE) did not use the correct amount of cellulose, plastic, and rubber (CPR) materials in DOE's MgO effective excess factor calculations (Brush and Roselle, 2006; Brush et al., 2006; Clayton and Nemer, 2006; Kanney and Vugrin, 2006; Vugrin et al., 2006) because DOE did not include the emplacement materials. EPA is correct that the 1.1×10^9 moles of organic carbon in CPR materials used the MgO analysis does not include the estimate of emplacement materials given in Burns (2005). The increased CPR inventory due to inclusion of the emplacement materials has the potential to affect not only the MgO effective excess factor calculations but also the 2004 Compliance Recertification Application (CRA-2004) Performance Assessment Baseline Calculation (PABC) (Leigh et al., 2005) and the Panel Closure Performance Assessment PA, (Vugrin and Dunagan, 2006). The impact of the change in total organic moles of CPR is explained for each analysis below. In all cases the impact to these analyses is minimal.

To correct this omission, six new parameters representing the density of CPR materials in emplacement materials will be created and used in future PAs. Table 1 lists the names, descriptions, units, and values of these parameters. Besides the emplacement material parameters, four additional parameters will be created that represent the density of cellulose and rubber materials in container (packaging) materials (Table 1). The addition of these parameters is done solely for book-keeping purposes since packaging materials do not contain cellulose or rubber materials. Future performance assessments will use the parameters in Table 1, in addition to the CRA-2004 PABC CPR parameters.

WIPP:1.4.1.:PA.QA-L:CPR Error : 543261
3/30/07 Rf

Information Only

Table 1. Cellulose, Plastic and Rubber Parameters to be created for the CRA-2009 PA¹

PROPERTY:MATERIAL	Description	Units	Parameter Type	Value
WAS_AREA:DPLSECHW	Average density of plastic in CH waste emplacement materials	kg/m ³	Constant	8.76
WAS_AREA:DPLSERHW	Average density of plastic in RH waste emplacement materials	kg/m ³	Constant	0
WAS_AREA:DCELECHW	Average density of cellulose in CH waste emplacement materials	kg/m ³	Constant	1.22
WAS_AREA:DCELERHW	Average density of cellulose in RH waste emplacement materials	kg/m ³	Constant	0
WAS_AREA:DRUBECHW	Average density of rubber in CH waste emplacement materials	kg/m ³	Constant	0
WAS_AREA:DRUBERHW	Average density of rubber in RH waste emplacement materials	kg/m ³	Constant	0

PROPERTY:MATERIAL	Description	Units	Parameter Type	Value
WAS_AREA: DCELCCHW	Average density of cellulose in CH waste container materials	kg/m ³	Constant	0
WAS_AREA: DCELCRHW	Average density of cellulose in RH waste container materials	kg/m ³	Constant	0
WAS_AREA: DRUBCCHW	Average density of rubber in CH waste container materials	kg/m ³	Constant	0
WAS_AREA: DRUBCRHW	Average density of rubber in RH waste container materials	kg/m ³	Constant	0

1. Here WAS_AREA:DPLSECHW and WAS_AREA:DCELECHW are calculated by dividing the mass from Table 2 in Section 1 by the volume available for contact-handled waste WAS_AREA:VOLCHW. All other materials listed in the table have no CPR contents and are assigned densities of 0 kg/m³.

1 CELLULOSE, PLASTIC, AND RUBBER INVENTORY

Below in Table 2 we give the amounts of cellulose, plastic, and rubber in the emplacement materials in kg and moles using the multiplicative factor of 1.7 for the plastics and a molecular weight of 6000/162 moles organic carbon per kg of cellulosic equivalent (Wang and Brush, 1996). Rubber has been left out of the table because Burns (2005) determined that emplacement materials contain little rubber.

Table 2. Total organic carbon of emplacement materials estimated by Burns (2005).

CPR Component	Total weight (kg)	Mass of cellulosic equivalent ¹ (kg)	Moles of organic carbon ² (moles)
Cellulose	2.07×10^5	2.07×10^5	7.67×10^6
Plastic	1.48×10^6	2.52×10^6	9.33×10^7
Total		2.73×10^6	1.01×10^8

1. Mass of cellulosic equivalent is calculated by multiplying the cellulose mass by 1 and the plastics mass by 1.7.

2. Moles of organic carbon is calculated by multiplying the mass of celluloses equivalent by a molecular weight of 6000/162 moles organic carbon/kg cellulosic equivalent.

In Table 3 we calculate the total organic carbon from non-emplacement materials. The data in Table 3 was obtained from the WIPP parameter database and is consistent to the values used in BRAGFLO calculations in the 2004-CRA PABC (Appendix A of Nemer and Stein, 2005)

Summing the total moles of organic carbon from Table 2-Table 3, we find that the total moles of organic carbon that should be used in the MgO Effective Excess Factor calculations is 1.21×10^9 , which rounds to 1.2×10^9 , to two significant digits. This CPR quantity is approximately 9 % higher than the CRA-2004 PABC value of 1.10×10^9 listed in Table 3.

Table 3. Cellulosics inventory from the CRA-2004 PABC. The volume of the contact-handled waste and the volume of the remote-handled waste were obtained from WAS_AREA:VOLCHW and WAS_AREA:VOLRHW respectively in the WIPP parameter database. The densities of CPR were also taken from the parameter database.

Type of cellulosics	contact (CH) or remote handled (RH)	WAS_AREA property in the parameter database	Density (kg/m ³)	Volume (m ³)	Mass of cellulosic equivalent ¹ (kg)
CELL	CH	DCELLCHW	60	1.69 x 10 ⁵	1.014 x 10 ⁷
-	RH	DCELLRHW	9.3	7080	6.5844x 10 ⁴
RUB	CH	DRUBBCHW	13	1.69 x 10 ⁵	2.197 x 10 ⁶
-	RH	DRUBBRHW	6.7	7080	4.7436 x 10 ⁴
PLAS	CH	DPLASCHW+DPLS CCHW	60	1.69 x 10 ⁵	1.7238 x 10 ⁷
-	RH	DPLASRHW+DPLS CRHW	11.1	7080	1.336 x 10 ⁵
-	Total	-	-	-	2.98219 x 10 ⁷
Total Moles organic C ²					1.10 x 10 ⁹

1. Mass of cellulosic equivalent is calculated by multiplying the cellulose mass by 1 and the plastics mass by 1.7. In this column we have kept sufficient significant digits to ensure that the resulting numbers are comparable to those produced by the ALGEBRA1 preprocessing step in the BRAGFLO calculations.

2. Moles of organic carbon is calculated by multiplying the mass of cellulosic equivalent by a molecular weight of 6000/162 moles organic carbon/kg cellulosic equivalent.

2 IMPACTS TO RELEVANT CRA-2004 PABC AND PANEL CLOSURE PA RESULTS

Dunagan et al., (2005) performed an analysis in which they compared total radionuclide releases from two PAs that differed only in CPR inventories; one PA had 2.5 times the CPR content of the other PA. Total releases were not significantly affected by the increased CPR inventory, and pressures, saturations and brine outflow were minimally affected. This minimal affect occurs because the primary impact on BRAGFLO simulations of a higher initial quantity of CPR is a higher rate of microbial gas production; the total fraction of CPR consumed in 10,000 years is weakly correlated to the amount of CPR available. Thus we do not believe that the additional CPR from the emplacement materials changes the results from either the CRA-2004 PABC or the panel closure PA (Vugrin and Dunagan, 2006). Nonetheless we give more detail below for the CRA-2004 PABC for the purpose of understanding the impact on the MgO Effective Excess Factor Calculations.

3 IMPACTS TO THE MGO EFFECTIVE EXCESS FACTOR CALCULATIONS

3.1 Impacts to relevant CRA-2004 PABC BRAGFLO results

The primary impact on BRAGFLO simulations of a slightly higher initial quantity of CPR is a slightly higher rate of microbial gas production. In the ALGEBRA1 step of the BRAGFLO computations, the sampled gas-generation rates are multiplied by the CPR density in the repository to arrive at the effective rate of gas generation per unit volume of repository; including the emplacement materials increases the CPR density by about 9% (1.2×10^9 versus 1.1×10^9 moles organic carbon/repository volume). To show the impact of slightly higher gas-generation rates, several plots of BRAGFLO results versus the inundated and humid gas-generation rates (in units of rate of gas generation per unit volume) have been prepared from CRA-2004 PABC results. In all cases the effect is small. Figure 1 shows the effect of the microbial gas-generation rate on the cumulative inflow of brine into the repository from the Castile brine pocket at 10,000 years, from scenario S2, replicate 1 from the CRA-2004 PABC.

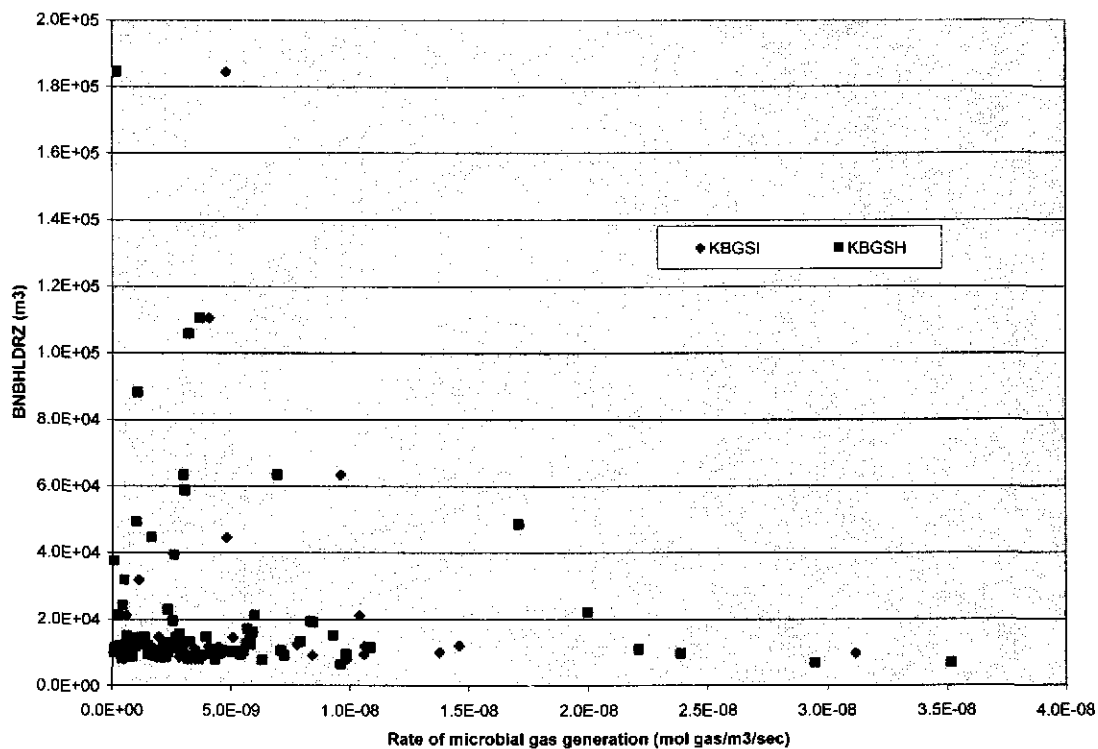


Figure 1. Plot of cumulative inflow of brine (m^3) into the repository from the Castile brine pocket BNBHLDRZ at 10,000 years versus the microbial gas-generation rates in ($\text{moles gas}/\text{m}^3 \text{ sec}$). Here KBGSI is the inundated gas-generation rate and KBGSH is the humid rate.

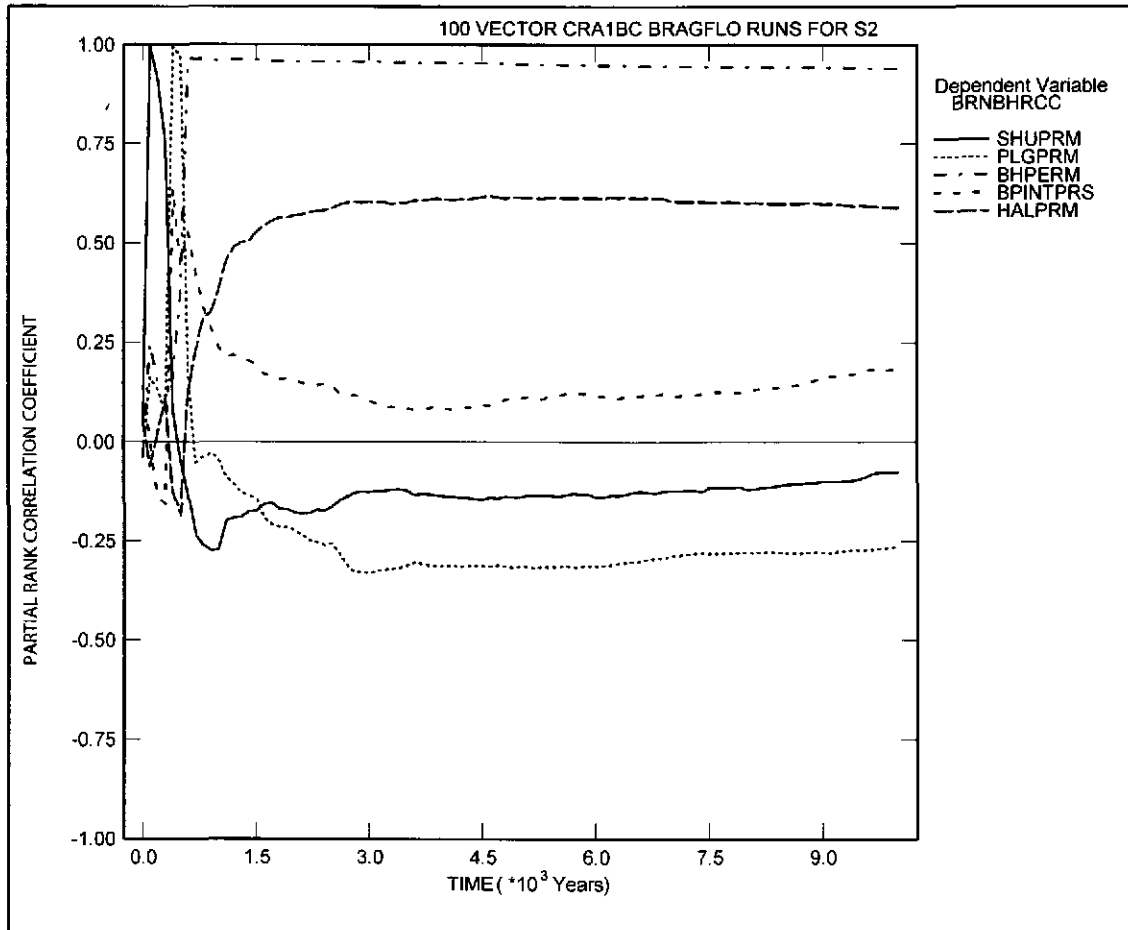


Figure 2. Primary Correlations for Cumulative Brine Flow Up the Borehole at the Culebra with Uncertain Parameters, Replicate R1, Scenario S2, from the CRA-2004 PABC.

Figure 1 indicates that the highest inflows of brine occurred for the lower gas generation rates. Figure 2 shows the results of regression analysis between the cumulative brineflow up the borehole to the Culebra (BRNBHRCC) and the uncertain BRAGFLO parameters in the analysis, for the CRA-2004 PABC. This plot is taken from Leigh et al. (2005). In Figure 2 none of the biodegradation variables appear, which is consistent the conclusion that the small difference in rates would not significantly affect brine flows.

Figure 3 shows the minimum porosity over 10,000 years for each vector versus the corresponding sampled rate of microbial gas-generation for that vector. The plot shows that the highest porosities occurred for both low and high microbial gas-generation rates.

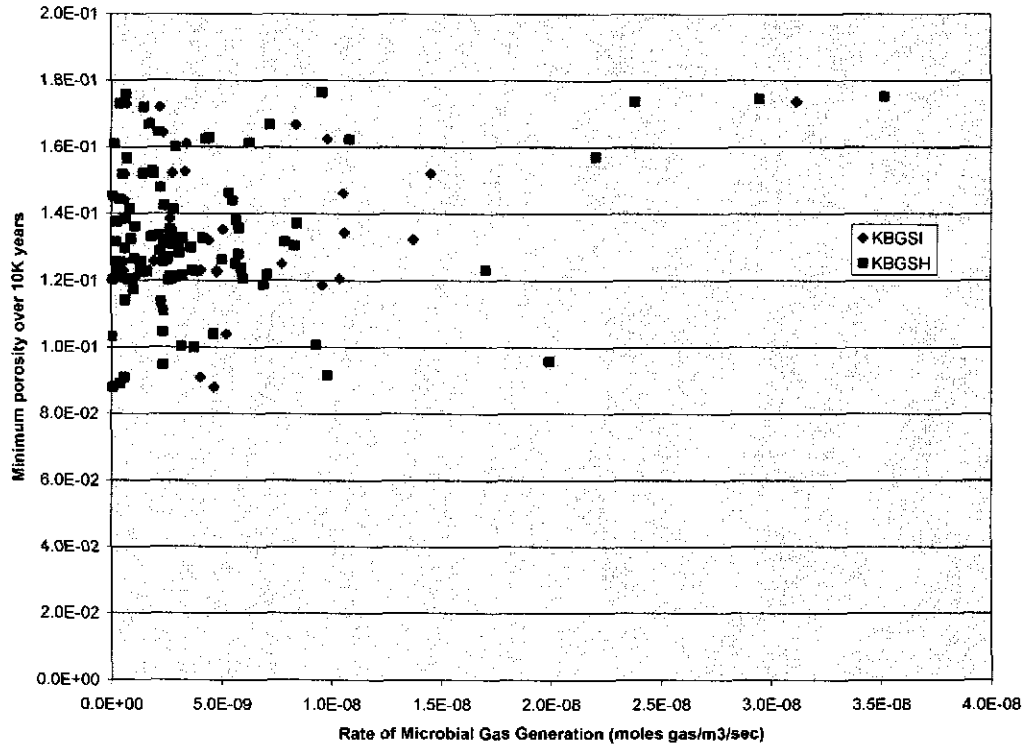


Figure 3. Plot of minimum porosity over 10,000 years for each vector versus the rate of microbial gas generation for scenario S2 of replicate R1 from the CRA1-PABC; labels are the same as in Figure 1.

3.2 Impacts to Individual MgO Effective Excess Factor Memos

The following analyses in the MgO Effective Excess Factor calculation memos and reports considered the CPR inventory:

Normalized moles of Castile sulfate entering the repository and fraction of MgO lost due to brine flow out of the repository (Clayton and Nemer, 2006).

Uncertainties Affecting MgO Effectiveness and Calculation of the MgO Effective Excess Factor (Vugrin et al., 2006).

Geochemical Information for Calculation of the MgO Effective Excess Factor (Brush and Roselle, 2006).

Consumption of Carbon Dioxide by Precipitation of Carbonate Minerals Resulting from Dissolution of Sulfate Minerals in the Salado Formation in Response to Microbial Sulfate Reduction in the WIPP (Brush et al., 2006).

Updated Analysis of Characteristic Time and Length Scales for Mixing Processes in the WIPP Repository to Reflect the CRA-2004 PABC Technical Baseline and the Impact of the Supercompacted Waste and Heterogeneous Waste Emplacement (Kanney and Vugrin, 2006).

The impact of the CPR increase on each analysis is discussed in the following subsections.

3.3 Impacts to Normalized moles of Castile sulfate entering the repository and fraction of MgO lost due to brine flow out of the repository (Clayton and Nemer, 2006).

As shown in Figure 1 and Figure 3, slightly higher gas-generation rates would have little effect on the amount of brine entering the waste area in an E1 intrusion. Thus the amount of sulfate entering the repository from the Castile and the amount of MgO lost to brine would not be significantly affected. Furthermore since Clayton and Nemer (2006) normalized the amount of sulfate from the Castile and the amount of MgO lost to brine by the total moles of organic carbon, we expect these ratios to decrease slightly. Therefore the current memo (Clayton and Nemer, 2006) would not be significantly affected with respect to the effect of increased CPR inventory.

3.4 Impact on Uncertainties Affecting MgO Effectiveness and Calculation of the MgO Effective Excess Factor (Vugrin et al., 2006).

The additional CPR from the emplacement materials affects this analysis quantitatively in three areas: the calculation of the variables y_{yield} and y_{L2B} and in Subsection 6.1 of Vugrin et al. (2006) which discusses the hydromagnesite to magnesite conversion.

3.4.1 Effective CO₂ yield (y_{yield})

When calculating y_{yield} from equation 4-7 in Vugrin et al., (2006), the terms F_D , F_{SW} , F_{SC} , are directly affected by the additional CPR from the emplacement materials. The terms F_D and F_{SW} can be recalculated given the 1.2×10^9 moles of organic carbon using equations 11-1 and 11-2 given in Appendix B. of Vugrin et al. (2006). Replacing 1.10×10^9 moles of organic carbon with 1.2×10^9 moles in Vugrin's equation 11-1, we find that denitrification (F_D) will now consume 0.0448 (as opposed to 0.0489). Replacing 1.10×10^9 moles of organic carbon with 1.2×10^9 in Vugrin's equation 11-2, we find that sulfate reduction using sulfates in the waste (F_{SW}) will consume 0.0077 (previously 0.0084) of the CPR inventory. These fractions are calculated in the same manner as described in Appendix B of Vugrin et al. (2006). Without re-running BRAGFLO calculations with the additional emplacement materials, we estimate the fraction of CPR materials that could be consumed via sulfate reduction with Castile sulfate (F_{SC}) by scaling the previous values (mean of 0.024 and standard deviation (SD) of 0.051) by 1.1/1.2, from which we find a mean of 0.022 and a standard deviation of 0.047. As

discussed above in Subsection 2, re-running BRAGFLO with the higher inventory will have little effect on CRA-2004 PABC results that affect F_{SC} .

The term F_{SM} in equation 4-7 of Vugrin et al. (2006) is multiplied by 0.69 moles CO_2 /1 mole consumed organic C, which is the amount of CO_2 that remains after consumption by calcium carbonate bearing minerals. The additional CPR due to the emplacement materials will not significantly impact this amount, as discussed in Subsection 3.8.

Given the results of the previous two paragraphs y_{yield} is determined to now have a mean of 0.713 and SD of 0.0146. This revised calculation proceeds in the same manner as detailed in Section 4.2.3 of Vugrin et al. (2006). These values were previously calculated to be 0.715 and 0.0158, respectively.

3.4.2 Loss of MgO to Brine Outflow (y_{L2B})

In calculating y_{L2B} , as discussed above in Subsection 2, we believe that re-running BRAGFLO would not significantly affect the loss of MgO to brine outflows. Furthermore y_{L2B} decreases with the increased CPR/MgO inventory because y_{L2B} is the ratio of the mass of MgO lost to brine outflows to the total amount of MgO emplaced. Thus it is reasonable to scale the previous results by the ratio 1.1/1.2. The previous mean and standard deviation were 0.008 and 0.019. The scaled mean and SD are 0.007 and 0.017.

3.5 Impacts to hydromagnesite to magnesite conversion

In equation 6-5 of Vugrin et al. (2006) the amount of uncarbonated Mg at time 0, and the rate of CO_2 production are all linearly dependent on the total initial inventory of organic carbon. The time at which all of the organic carbon is consumed in equation 6-8 of Vugrin et al. (2006), $t_{all\ CPR}$, is not a function of the total inventory of organic carbon because the inventory of organic carbon scales out of this equation. It follows then that the fraction of MgO remaining at $t_{all\ CPR}$ is independent of the total inventory of organic carbon, and thus Figures 3 and 4 in Vugrin et al. (2006) remain unchanged. The conclusions and numbers presented in Subsection 6.1 of Vugrin et al. (2006) also remain unchanged.

3.6 Impacts to EEF

Using the recalculated values for y_{L2B} and y_{yield} from Subsections 3.4.1-3.5, the mean effective excess factor (EEF) is unchanged to 3 significant digits (1.60). The standard deviation decreased from 0.0819 to 0.077. Thus there is no impact of the increased CPR inventory upon the conclusions reached in Vugrin et al., (2006).

3.7 Impacts to Geochemical Information for Calculation of the MgO Effective Excess Factor (Brush and Roselle, 2006)

Subsection 6.1 of Brush and Roselle (2006) discusses the total inventory of organic carbon, total possible CO₂ produced and total possible H₂S produced. The number 1.1×10^9 moles of organic carbon written in that subsection (and elsewhere in the report) should be replaced by 1.2×10^9 moles. Subsection 6.1 of Brush and Roselle (2006) also refers to and uses the fractions F_D , and F_{SW} . These values should be replaced by those given above in Subsection 3.4.1. Using these numbers and the same calculation methods as given in Brush and Roselle (2006), the maximum amount of H₂S that could be produced is now 5.73×10^8 moles (compared to 5.24×10^8 moles using 1.1×10^9 moles organic C). This number is calculated by assuming that after denitrification, all microbial CPR consumption occurs through sulfate reduction. Then the amount of H₂S produced will be $0.5 \times (1 - F_D) \times 1.2 \times 10^9$ moles CPR, where the 0.5 factor is the moles of H₂S produced per mole of organic carbon consumed (see equation 13 of Brush and Roselle, 2006). Therefore the minimum quantity of CO₂ that could be consumed by carbonation of steels and other Fe-base metals (9.21×10^8 moles Fe) is 9.21×10^8 moles – 5.73×10^8 moles = 3.48×10^8 moles (compared to 3.97×10^8 moles) which corresponds to 29.0 % of the total CO₂ that could be produced by complete microbial consumption of all CPR in the repository (compared to 36.1 %).

Subsection 6.2 of Brush and Roselle (2006) analyzes lead (Pb) analogously to Subsection 6.1. Using the larger quantity of CPR we find that lead could consume 1.25 % of the CO₂ that could be produced by complete microbial consumption of all CPR in the repository (compared to 1.36 %). The total consumption of CO₂ by metals is now 30.25 % (compared to 37.5 %). These percentages are calculated by multiplying the previous percentages by the ratio 1.1/1.2.

Subsection 6.3 Brush and Roselle (2006) analyzes portlandite analogously to Subsection 6.1-6.2. Using the larger quantity of CPR we find that the free lime and Portland cements could consume 0.163 % of the CO₂ that could be produced by complete microbial consumption of all CPR in the repository (compared to 0.177 %). This percentage is calculated by multiplying the previous percentage by the ratio 1.1/1.2.

Because the amount of CO₂ that could be dissolved in brine (Subsection 6.4 Brush and Roselle, 2006) is so small, here we do not bother to update this portion of the analysis.

3.8 Impact to Consumption of Carbon Dioxide by Precipitation of Carbonate Minerals Resulting from Dissolution of Sulfate Minerals in the Salado Formation in Response to Microbial Sulfate Reduction in the WIPP (Brush et al., 2006)

We have not found any reason why increasing the CPR inventory by 9 % would significantly change the brine compositions, the relative percentage of carbonate minerals precipitated, or the effective CO₂ yields. The only affect that we have identified is that

the amount of DRZ that would be required to supply sulfate for sulfate reduction, of the 95 % of organic carbon remaining after denitrification and sulfate reduction using the sulfate in the waste, would increase from 45 % to 49 % (multiplying by 1.2/1.1).

3.9 Impacts to Updated Analysis of Characteristic Time and Length Scales for Mixing Processes in the WIPP Repository to Reflect the CRA-2004 PABC Technical Baseline and the Impact of the Supercompacted Waste and Heterogeneous Waste Emplacement (Kanney and Vugrin, 2006).

Based on the discussion in Subsection 2, the additional CPR would have little impact on the minimum porosity and the maximum brine flow rates. Therefore we expect that the results of Kanney and Vugrin (2006) would not be significantly affected.

4 CONCLUSIONS

Based on the discussion above we conclude that inclusion of the emplacement CPR materials would have little quantitative or qualitative effect on the conclusions made in the MgO effective excess factor calculations (Vugrin et al., 2006), the CRA-2004 PABC (Leigh et al., 2005), and the Panel Closure PA (AP129) (Vugrin and Dunagan, 2006)

5 REFERENCES

- Brush, L. H. and G. T. Roselle. 2006. "Geochemical Information for Calculation of the MgO Excess Factor." Report, November 17, 2006. Carlsbad, NM: Sandia National Laboratories. ERMS 544840.
- Brush, L. H., Y.-L. Xiong, J. W. Garner and A. Ismail. 2006. "Consumption of Carbon Dioxide by Precipitation of Carbonate Minerals Resulting from Dissolution of Sulfate Minerals in the Salado Formation in Response to Microbial Sulfate Reduction in the WIPP." Report, November 17, 2006. Carlsbad, NM: Sandia National Laboratories. ERMS 544785.
- Burns, T. 2005. "Estimation of Cellulose, Plastic, and Rubber Based on TWBID, Rev. 2.1, Data Version 4.15." Report, January 26, 2005. Carlsbad, NM: Los Alamos National Laboratory. ERMS 538664.
- Clayton, D. J. and M. B. Nemer. 2006. "Normalized Moles of Castile Sulfate Entering the Repository and Fraction of MgO Lost Due to Brine Flow Out of the Repository." Report, October 9, 2006. Carlsbad, NM: Sandia National Laboratories. ERMS 544385.

- Dunagan, S., C. Hansen and W. Zelinski. 2005. "Effect of Increasing Cellulosics, Plastics, and Rubbers on WIPP Performance Assessment." Report, January 18, 2005. Carlsbad, NM: Sandia National Laboratories. ERMS 538445.
- Kanney, J. F. and E. D. Vugrin. 2006. "Updated Analysis of Characteristic Time and Length Scales for Mixing Processes in the WIPP Repository to Reflect the CRA-2004 PABC Technical Baseline and the Impact of the Supercompacted Mixed Waste and Heterogeneous Waste Emplacement." Report, August 31, 2006. Carlsbad, NM: Sandia National Laboratories. ERMS 544248.
- Leigh, C., J. Kanney, L. Brush, J. Garner, R. Kirkes, T. Lowry, M. Nemer, J. Stein, E. Vugrin, S. Wagner and T. Kirchner. 2005. "2004 Compliance Recertification Application Performance Assessment Baseline Calculation." Report, October 19, 2005. Carlsbad, NM: Sandia National Laboratories. ERMS 541521.
- Nemer, M. B. and J. S. Stein. 2005. "Analysis Package for BRAGFLO: 2004 Compliance Recertification Application Performance Assessment Baseline Calculation." Analysis Report, June 28, 2005. Carlsbad, NM: Sandia National Laboratories. ERMS 540527.
- Vugrin, E. and S. Dunagan. 2006. "Analysis Package for the Impact Assessment of the Redesigned WIPP Panel Closure, Revision 0." Analysis Report, July 7, 2006. Carlsbad, NM: Sandia National Laboratories. ERMS 543865.
- Vugrin, E. D., M. B. Nemer and S. Wagner. 2006. "Uncertainties Affecting MgO Effectiveness and Calculation of the MgO Excess Factor." Report, November 17, 2006. Carlsbad, NM: Sandia National Laboratories. ERMS 544781.
- Wang, Y. and L. Brush. 1996. "Modify the Stoichiometric Factor y in BRAGFLO to Include the Effect of MgO Added to the WIPP Repository As a Backfill." Memorandum to Martin S. Tierney Albuquerque, NM: Sandia National Laboratory. ERMS 232286.